NATIONAL TRANSPORTATION SAFETY BOARD
Office of Aviation Safety
Washington, D.C. 20594

May 2, 2012

Computed Tomography Specialist's Factual Report

DCA12MA020

A. INCIDENT

Operator:	Sundance Helicopters
Location:	Approximately 14 miles east of Las Vegas, NV
Date:	December 7, 2011
Time:	1630 Pacific Standard Time
Airplane:	Eurocopter AS350-B2, N37SH

B. GROUP

Computed Tomography Specialist: Scott Warren
National Transportation Safety Board
Washington, D.C.

C. SUMMARY

On December 7, 2011 at 1630 Pacific Standard Time, a Eurocopter AS350-B2, registration N37SH, operated by Sundance Helicopters as flight Landmark 57, crashed in mountainous terrain approximately 14 miles east of Las Vegas, Nevada. The 14 CFR Part 135 flight was a tourist sightseeing flight, which departed from Las Vegas McCarren International Airport (LAS), Las Vegas, NV, intending to fly to the Hoover Dam area and return to LAS, operating under visual flight rules. The helicopter impacted in a narrow ravine in mountainous terrain between the city of Henderson and Lake Mead. The pilot and four passengers were fatally injured, and the helicopter was substantially damaged by impact forces and post-crash fire. Weather was reported as clear with good visibility and dusk light conditions.

Radar data obtained from the FAA show that the helicopter departed LAS and followed a normal route of flight easterly out of the LAS airport traffic area, then turned to the southeast toward Hoover Dam. Tour routings are standardized for all the area tour operators. The helicopter was level at 3,500 feet mean sea level (MSL) at approximately 120 knots. About one minute prior to the accident, the radar indicated the helicopter climbed to 4,100 feet MSL and turned about 90 degrees to the left. The left turn and climb are not part of the normal route. Radar then indicated the helicopter descended to 3,300 feet MSL and tracked a northeasterly course for about 20 seconds, until entering a left turn then a descent. The last radar target received was about 1/8 miles from the accident site.

Radiographic studies were done on January 25-31, 2012 in Chicago, Illinois to examine and document the internal configuration of the main rotor and tail rotor actuators. The actuators were documented using a combination of computed tomography (CT) scans and digital radiography. The actuators were imaged using a total of 18 digital radiographs (DR) and 3,435 CT slices. In addition, a rod end of the fore-aft actuator was imaged using 2 DR's and 928 CT slices.

There was an apparent ribbon of unknown material found in the images of the fore-aft actuator. There were particles found in the images for both the left lateral and tail rotor actuators. The location for the internal filter within the right lateral actuator was noted to be empty. No anomalies were noted in the rod end of the fore-aft actuator.

D. DETAILS OF THE INVESTIGATION

1.0 General

The actuators were subjected to x-ray computed tomography (CT) and digital radiography scanning to document the internal conditions of all of the actuators. In addition, one of the fore-aft actuator rod ends was scanned using a microfocus CT process. The scans were performed by Varian Medical Systems, Inc (formerly Bio-Imaging Research, Inc. (BIR)) under the direction of the NTSB.

To conduct the scans, Varian used an ACTIS 800/450-225 CT system with either a 450 kV source for the actuators and a 225 kV MicroFocus source for the fore-aft actuator rod end using an x-ray source strength of 445 kV and 2 mA for the actuators and 220 kV and 450 µA for the fore-aft actuator rod end. The system recorded the x-ray attenuation information using either a liner array (actuators) or a Perkins-Elmer flat panel (fore-aft actuator rod end) detector system.

For the CT scans, the actuators were loaded individually into the imaging unit and placed on a turntable. The assembly was then rotated in front of the x-ray source, and the x-rays were captured by a detector after they went through the assembly. The x-ray source produced a fan beam of x-rays (or a cone of x-rays in the case of the microfocus source), and the portion of the assembly imaged by x-rays was adjusted slightly after each slice or scan volume was completed until the entire assembly (or region of interest of the assembly) was scanned. The x-ray energy levels captured by the detector were recorded at 1,440 different points during each rotation for the actuators and 3,600 different points during each rotation for the fore-aft actuator rod end, and this information was converted into slice images using reconstruction algorithms.

A total of 3,435 CT slices were gathered to document all of the actuators. Each slice was 2,048 x 2,048 pixels wide and had a resulting image file size of slightly over 8 megabytes (Mb). For the actuators, the slices were created with a thickness of 0.50 mm at a spacing of 0.40 mm with a cross sectional pixel dimension within each slice of approximately 0.122 mm x 0.122 mm. For the fore-aft actuator rod end, a total of 928 slices were gathered with a thickness of 0.070 mm at a spacing of 0.023 mm with a cross sectional pixel dimension within each slice of approximately 0.0229 mm x 0.0229 mm.

For the digital radiograph (DR) images, the assembly was subjected to a process similar to a conventional x-ray. The image was gathered using the same detector used for the CT scans, but the assembly did not rotate, and the images contain elements superimposed on each other. Each filter was imaged at least twice, and the separate images were obtained at positions rotated by up to 90 deg.

Each data set of CT slice images was evaluated using the VGStudio Max software package to either view the individual slices in detail or to create a three-dimensional reconstructed image of the component. As part of the evaluation, some sections of the actuators were digitally removed to allow closer observation of interior parts.

For this study, computing limitations precluded loading the complete data set into VGStudio Max at one time. The actuators were examined in segments consisting of approximately one half of the actuator in each segment.

The images of the actuators were examined for any signs of missing or damaged parts, contamination, or any other anomalies. Specific results (including example images) are presented in subsequent sections of this report.

2.0 Digital Radiograph Results

Digital radiograph images from all of the actuators and the fore-aft actuator rod end are shown in figures 1 through 8. No particles or other defects were noted in any of the digital radiographs.

Figure 1
Digital Radiograph – Fore-Aft Actuator

Figure 2
Digital Radiograph – Fore-Aft Actuator, rotated view

Figure 3
Digital Radiograph – Right Lateral Actuator

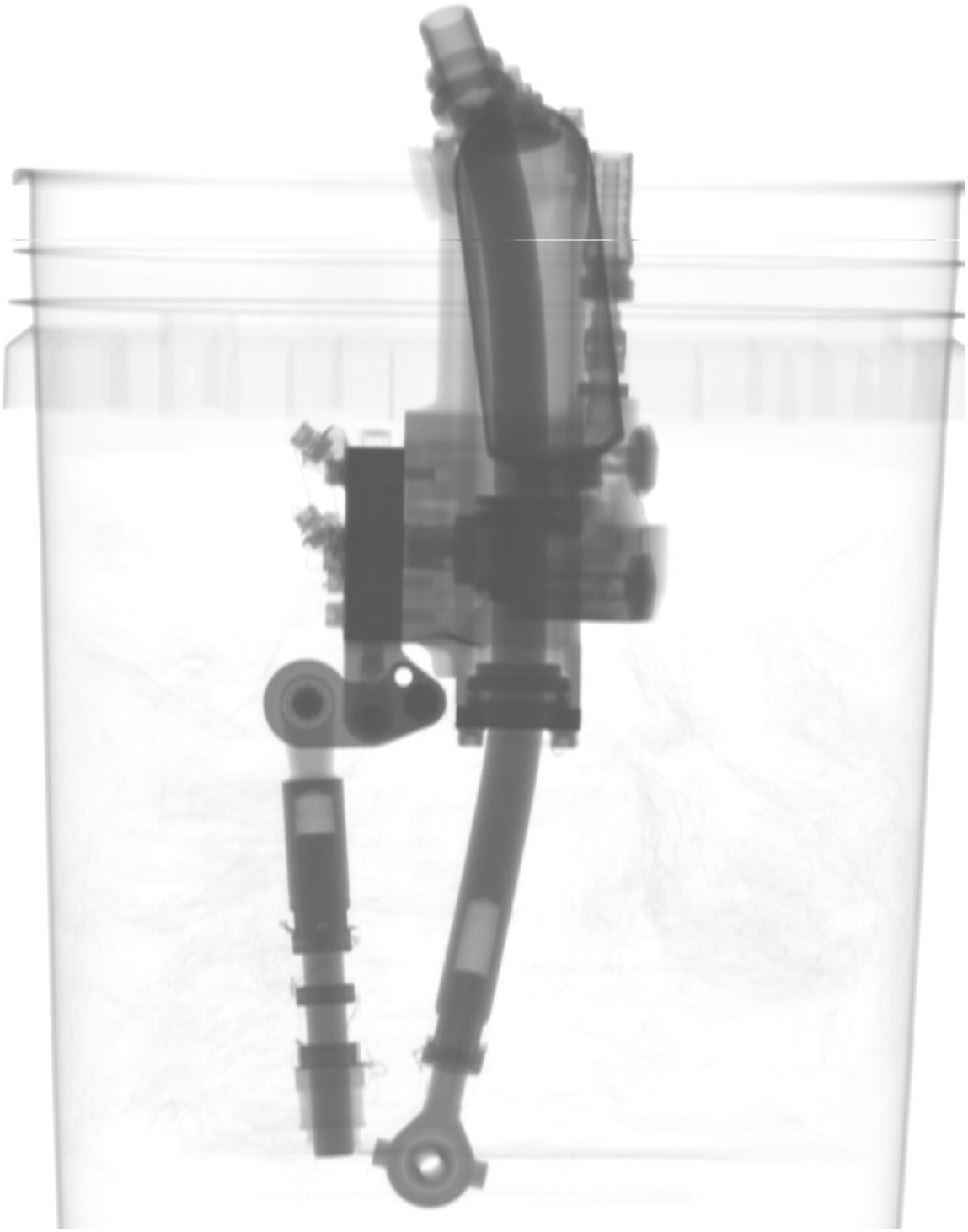

Figure 4
Digital Radiograph – Right Lateral Actuator, rotated view

Figure 5
Digital Radiograph – Left Lateral Actuator

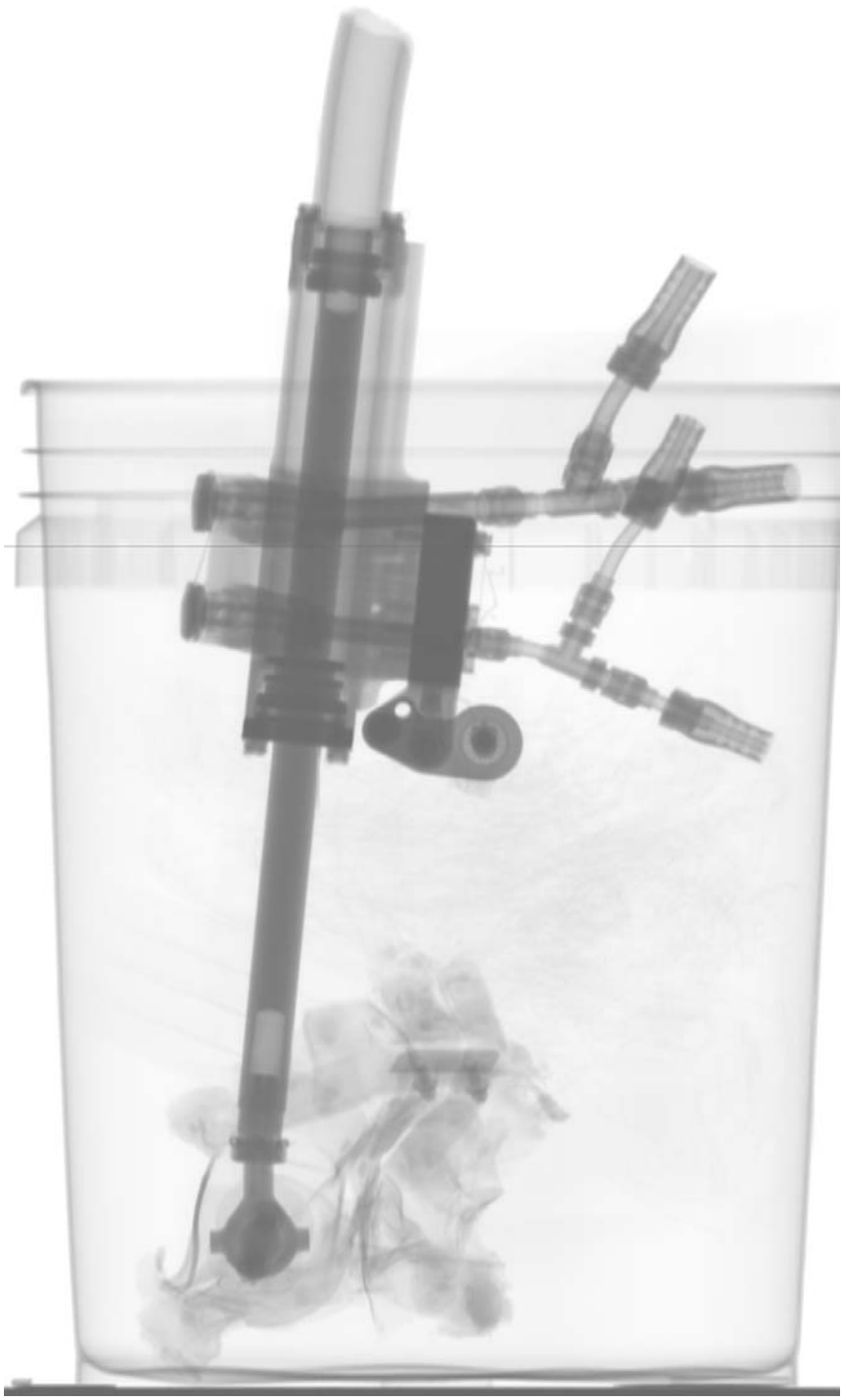

Figure 6
Digital Radiograph – Tail Rotor Actuator

Figure 7
Digital Radiograph – Fore-Aft Actuator Rod End

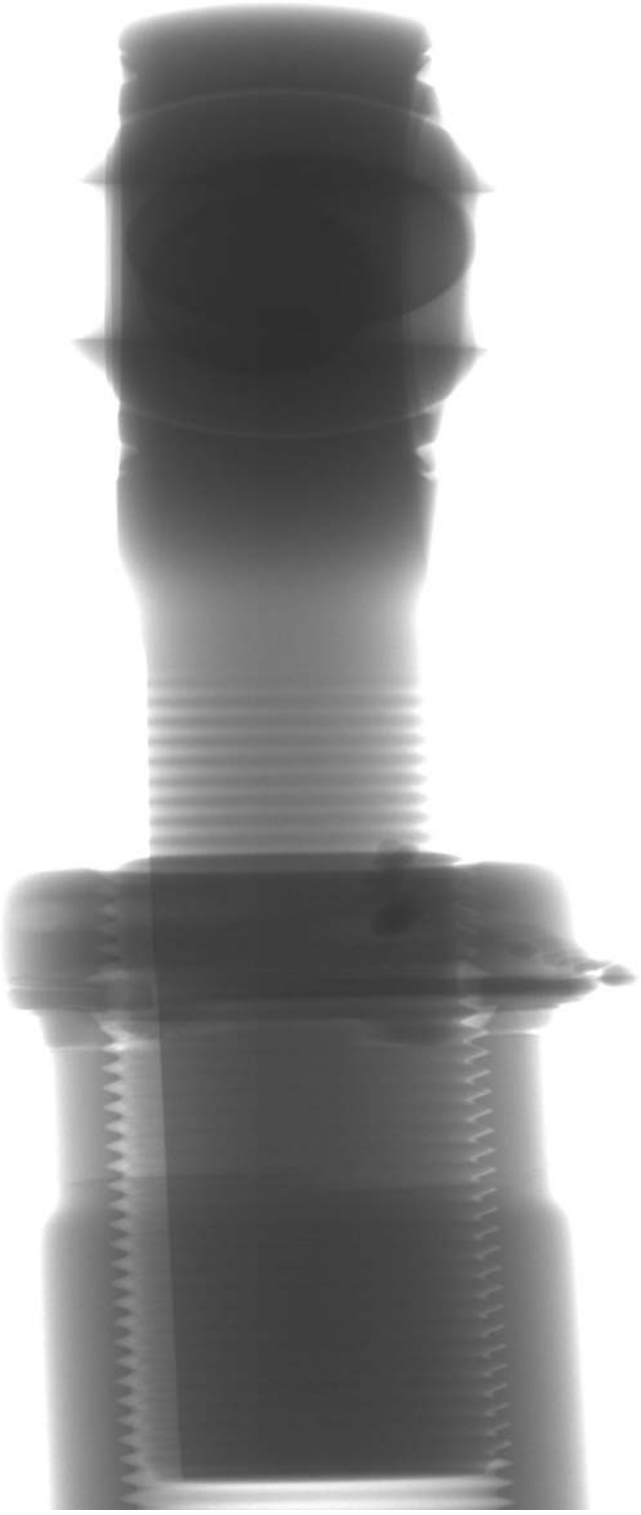

Figure 8
Digital Radiograph – Fore-Aft Actuator Rod End, Rotated View

3.0 Computed Tomography Results – Fore-Aft Actuator

The computed tomography (CT) results for the fore-aft actuator are shown in figures 9 through 13. A ribbon of unknown material was noted above and below the piston head of the actuator. A nominal thickness for the ribbon was measured to be approximately 3.19 mm.

No other anomalies were noted in the actuator. The lock plunger for the actuator appeared to be in the engaged position within the lever assembly.

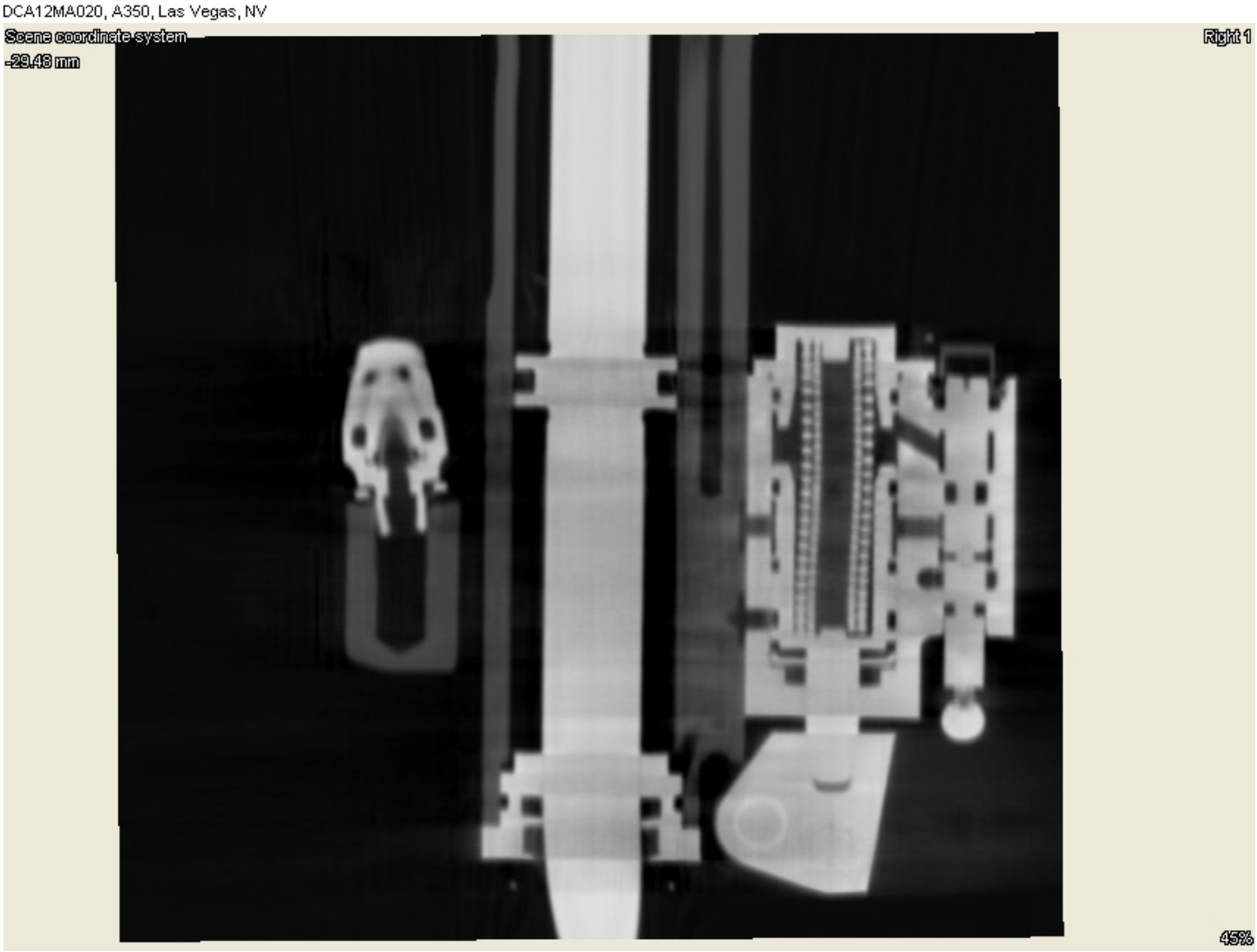

Figure 9
Right cross section – Fore-Aft Actuator – Overall cross sectional view of the actuator showing the positions of the lock plunger, spool, and piston head

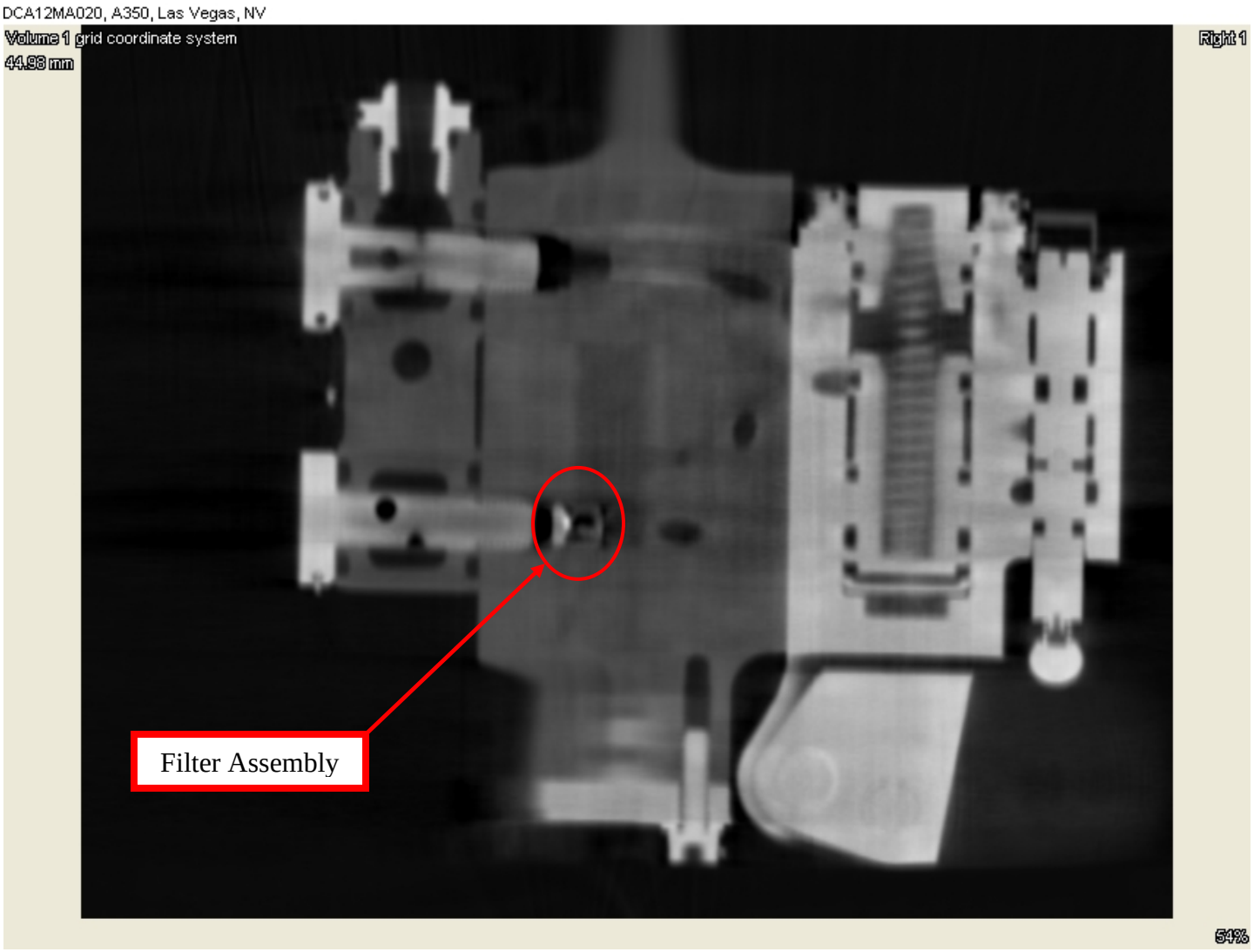

Figure 10
Right cross section – Fore-Aft Actuator – Cross sectional view of the actuator showing the filter assembly

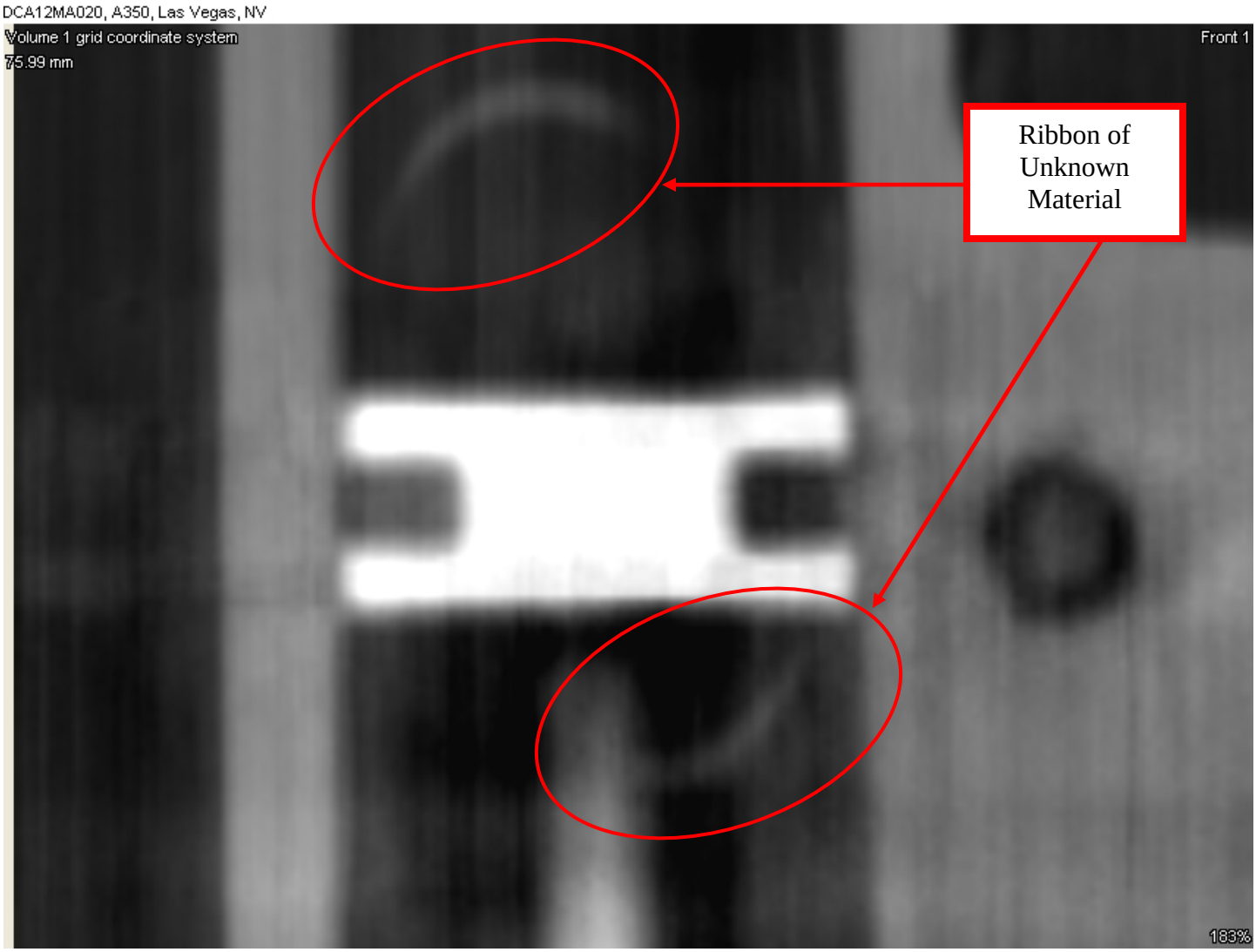

Figure 11
Frontal cross section – Fore-Aft Actuator – Apparent ribbon of unknown material above and below the piston head of the actuator

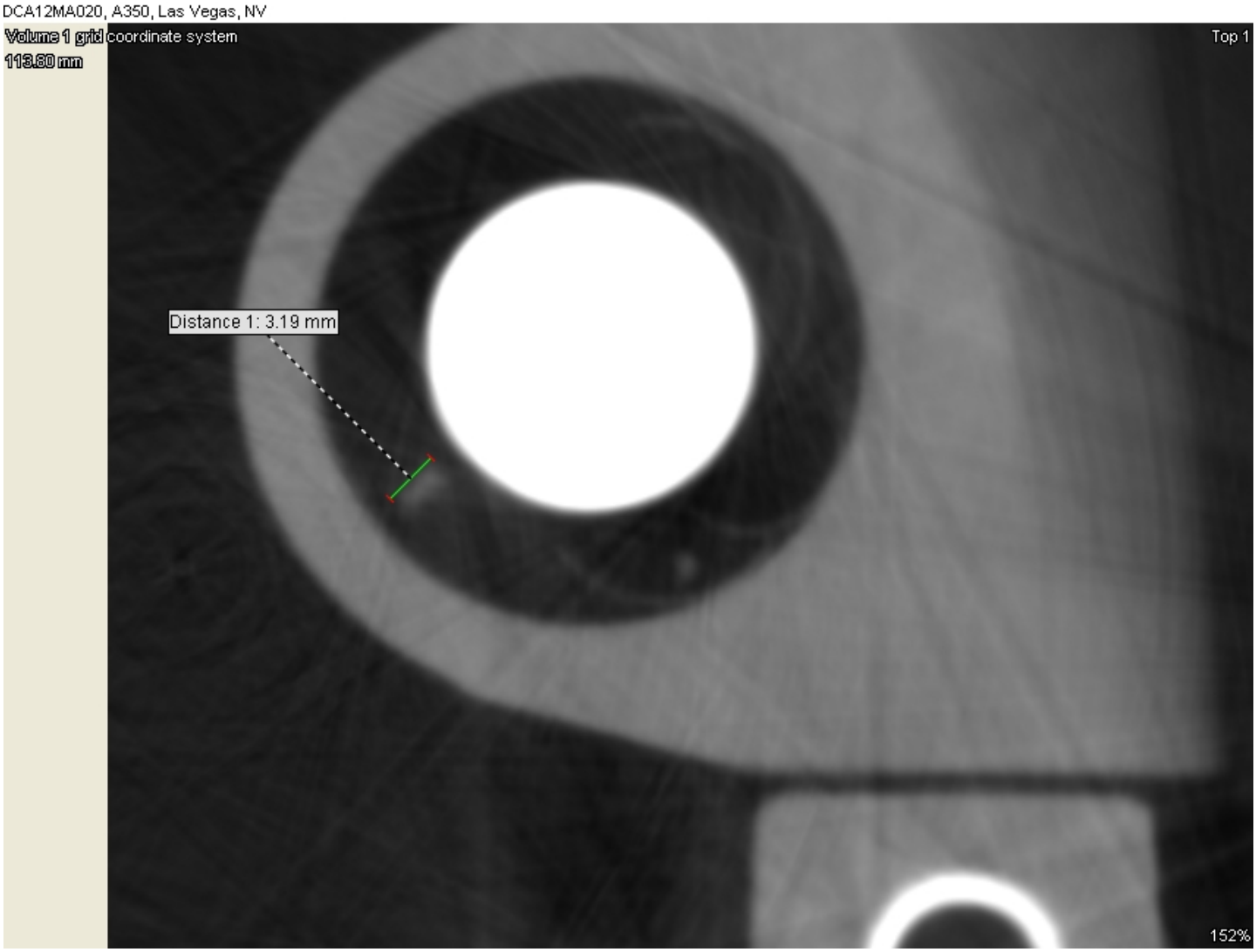

Figure 12
Axial cross section – Fore-Aft Actuator – Thickness of apparent ribbon of unknown material measuring 3.19 mm

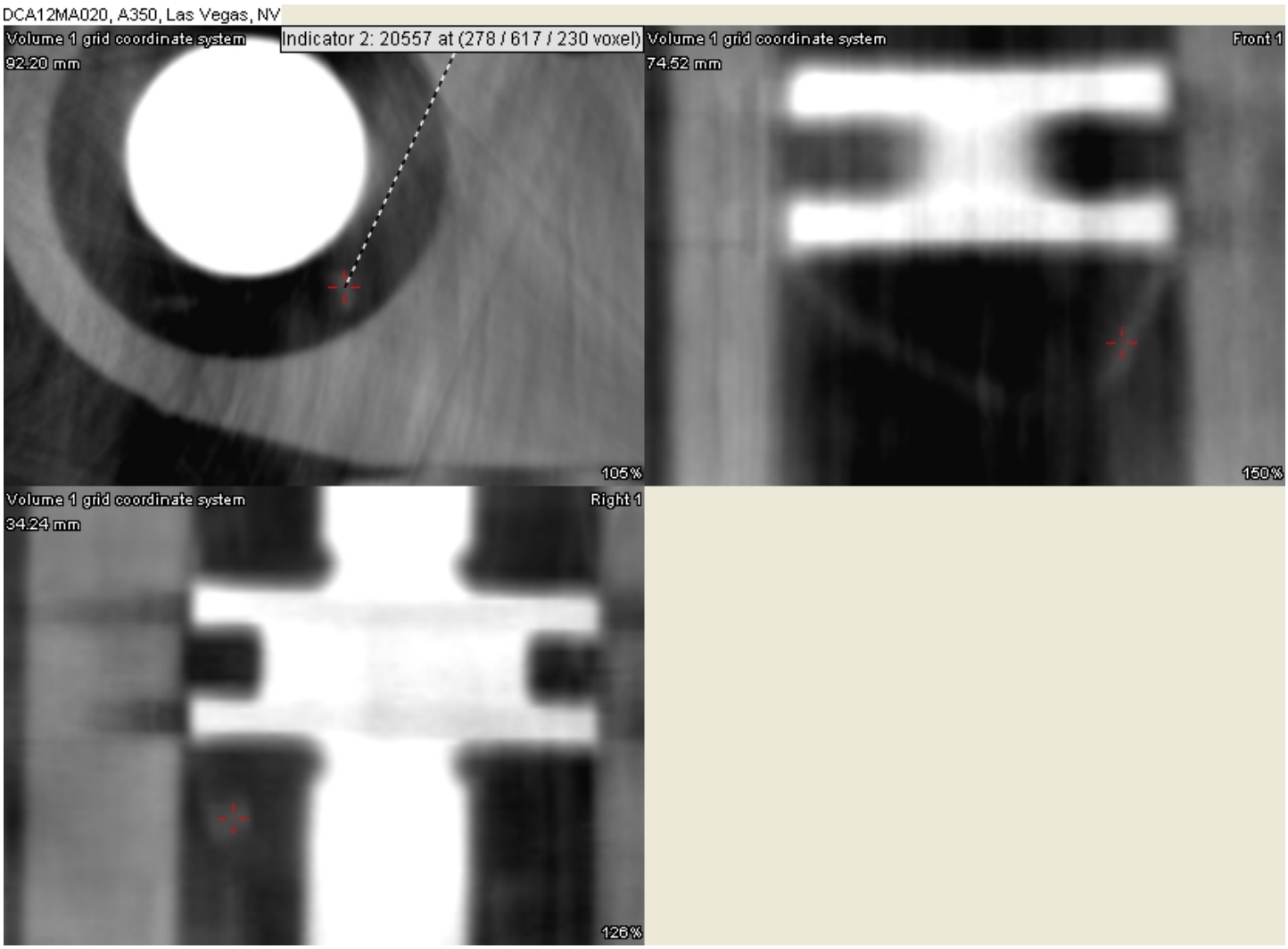

Figure 13
Multiple views – Fore-Aft Actuator – Apparent ribbon of unknown material below the piston head of the actuator

4.0 Computed Tomography Results – Left Lateral Actuator

The computed tomography (CT) results for the left lateral actuator are shown in figures 14 through 21. A total of four particles were found in various locations within the actuator.

Figure 14
Multiple views – Left Lateral Actuator – Overall cross section showing shuttle position

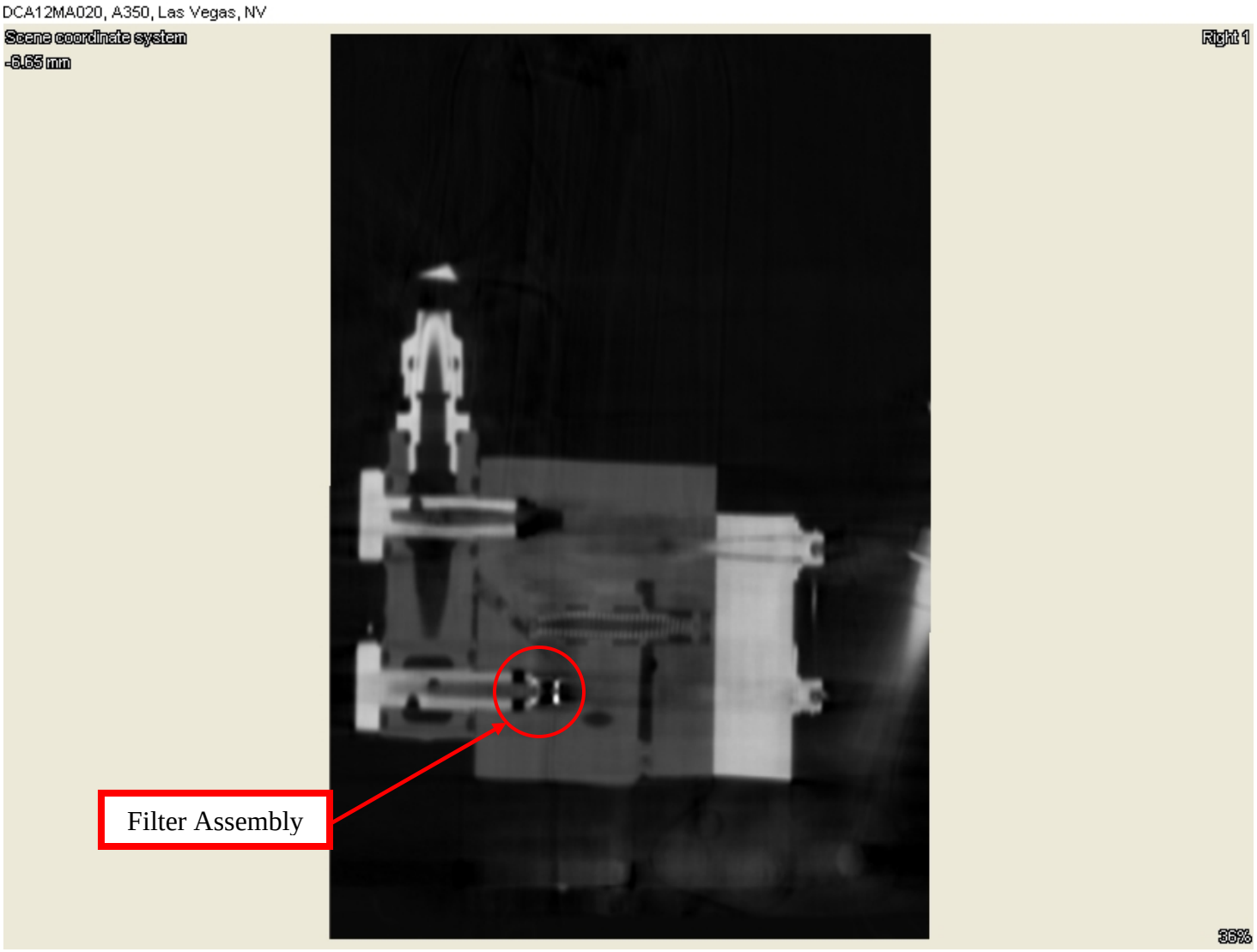

Figure 15
Right cross section – Left Lateral Actuator – Overall cross section showing pressure and return ports and filter

Figure 16
Multiple views – Left Lateral Actuator – Cross sectional views of the actuator showing the position of the spool

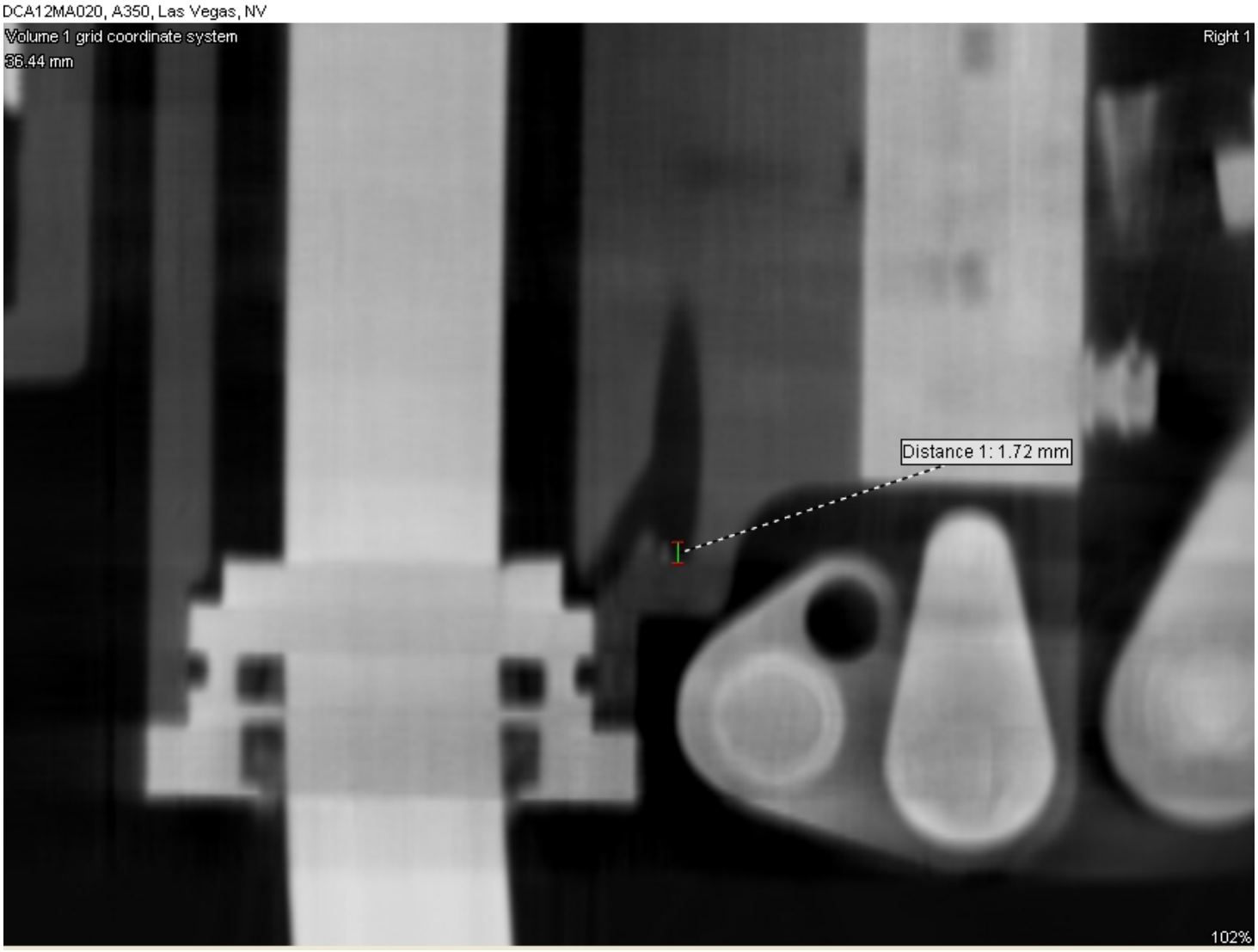

Figure 17
Right cross section – Left Lateral Actuator – Particle, measuring 1.72 mm long, at the end of a hydraulic passage

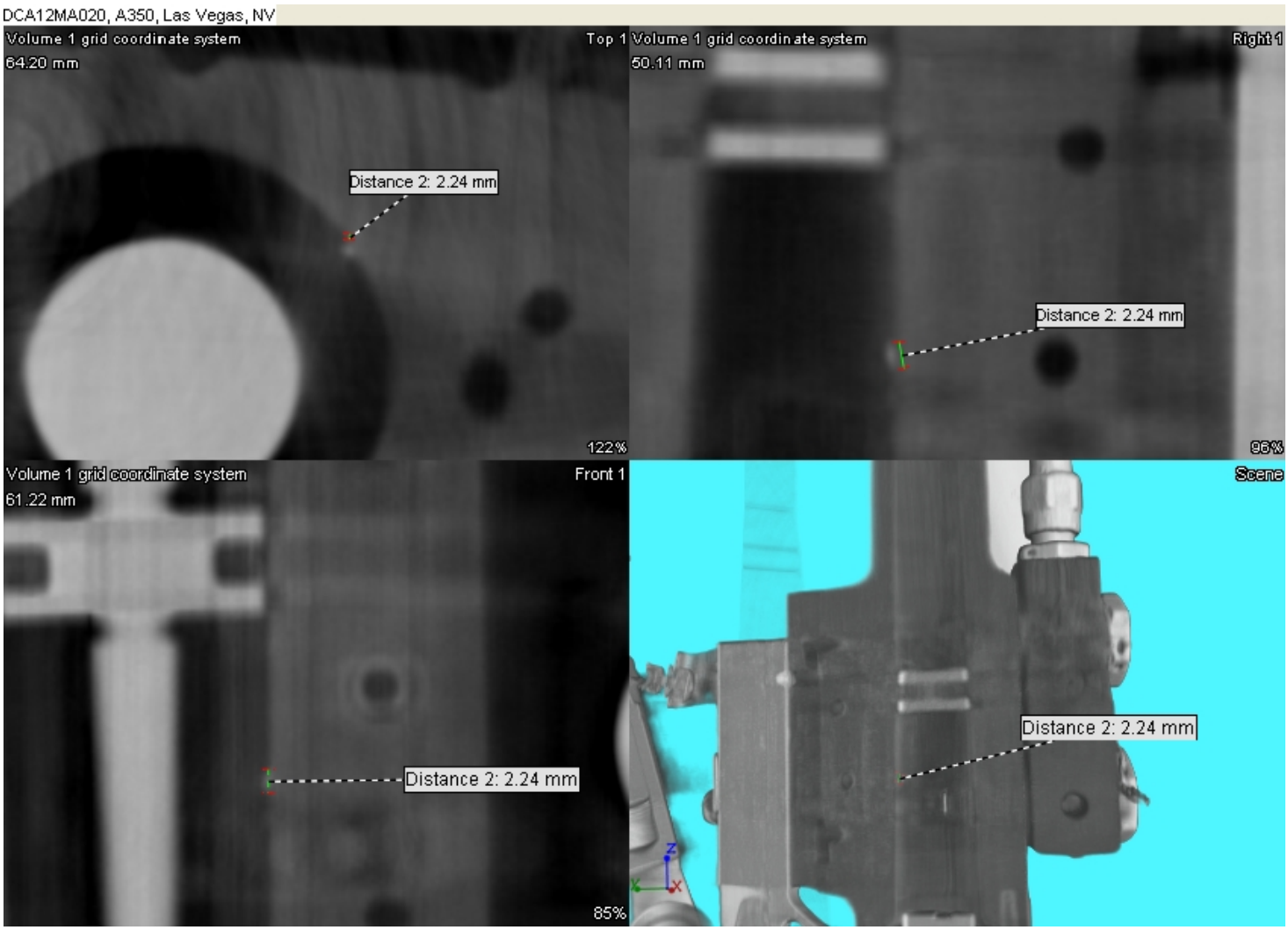

Figure 18
Multiple views – Left Lateral Actuator – Particle 2, measuring 2.24 mm long, on the wall of the piston cavity

Figure 19
Frontal cross section – Left Lateral Actuator – Particle 3, measuring 1.72 mm long, at the end of a hydraulic passage adjacent to the spool

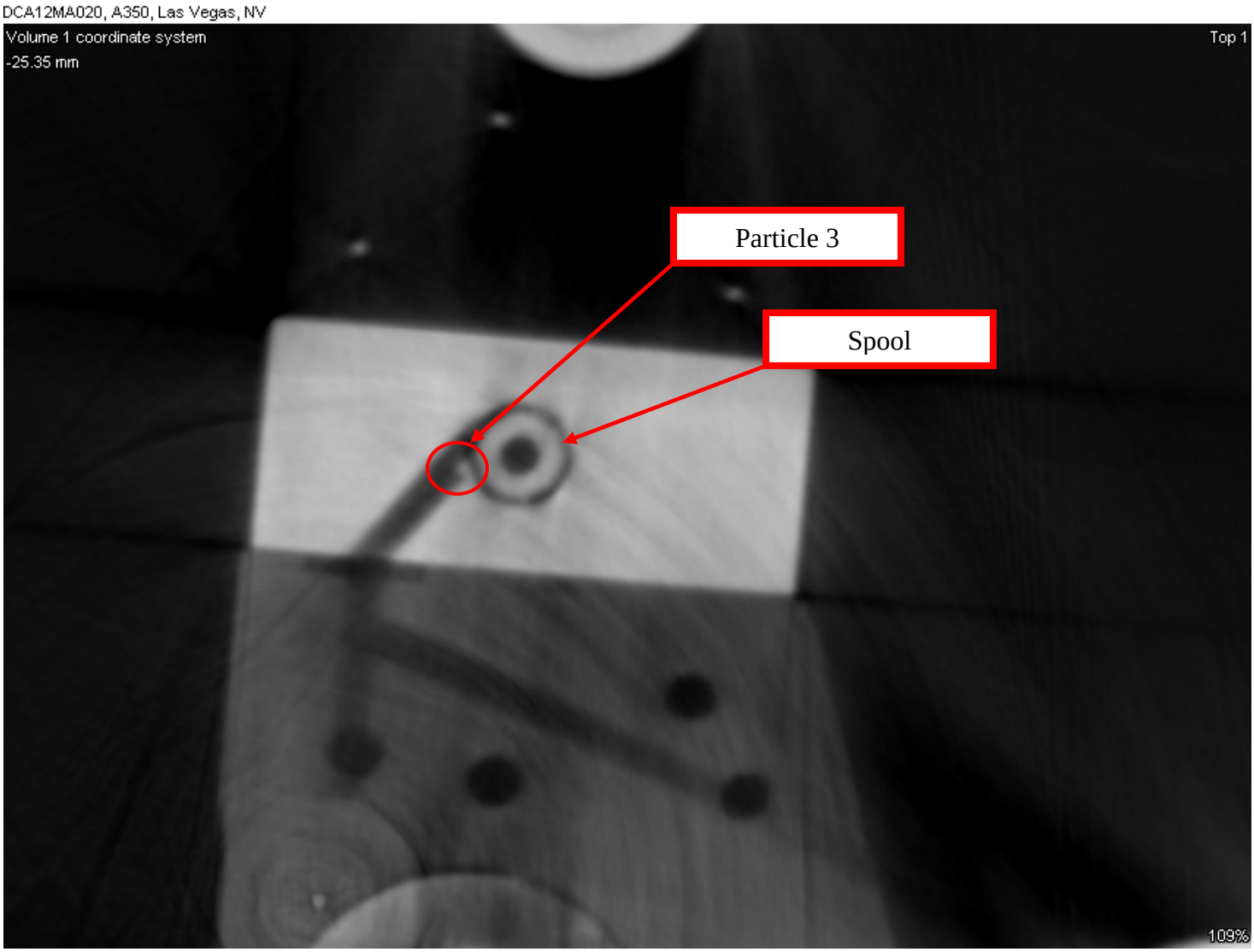

Figure 20
Axial cross section – Left Lateral Actuator – Particle 3, measuring 1.72 mm long, at the end of a hydraulic passage adjacent to the spool

Figure 21
Right cross section – Left Lateral Actuator – Particle 4, measuring 1.50 mm long, at the end of a hydraulic passage

5.0 Computed Tomography Results – Right Lateral Actuator

The computed tomography (CT) results for the right lateral actuator are shown in figures 22 through 24. No particles were found in this actuator, however there was no filter visible in the pressure port area.

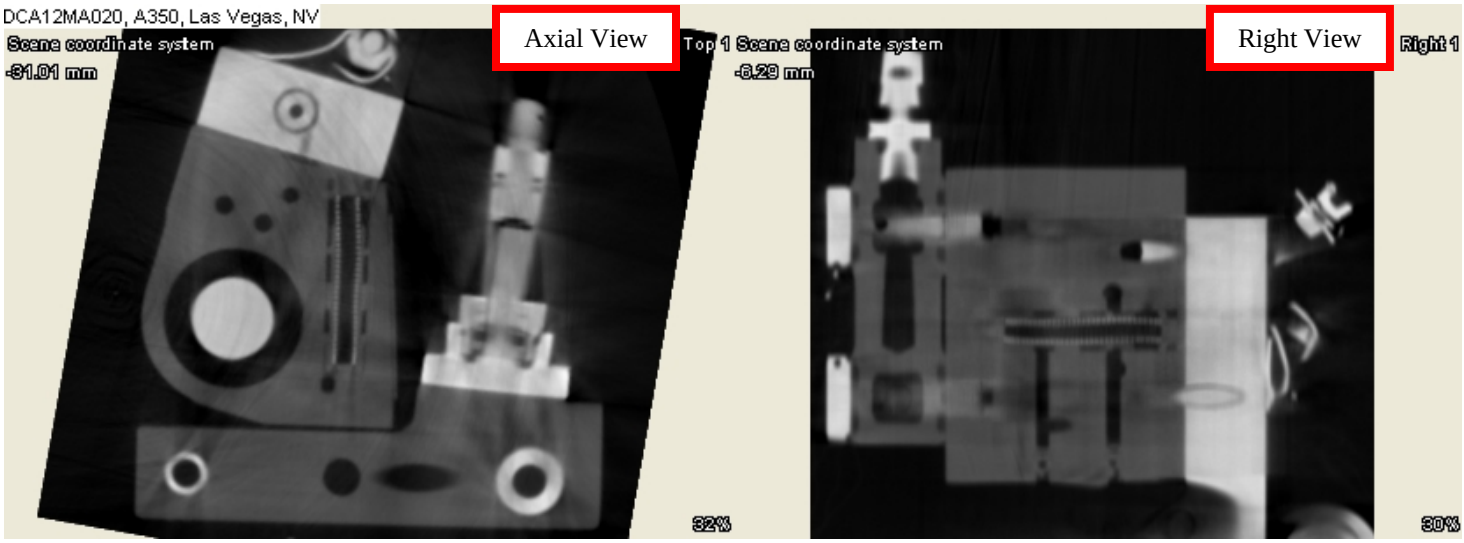

Figure 22
Multiple views – Right Lateral Actuator – Overall cross section showing the shuttle position

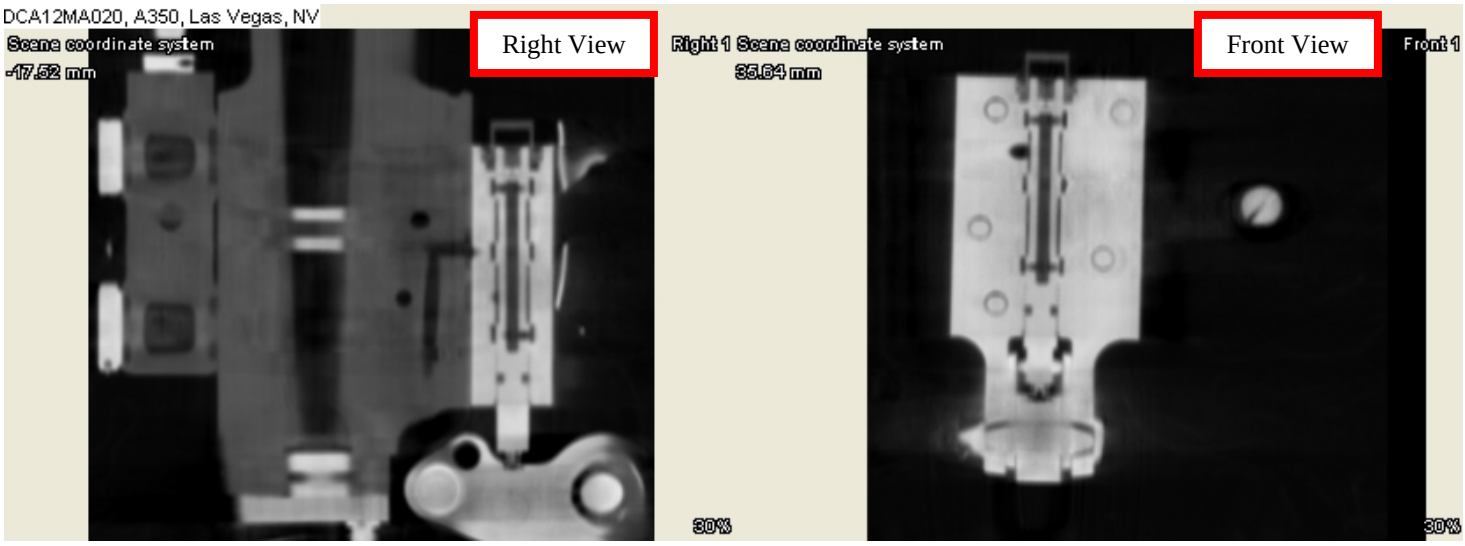

Figure 23
Multiple views – Right Lateral Actuator – Overall cross section showing the spool position

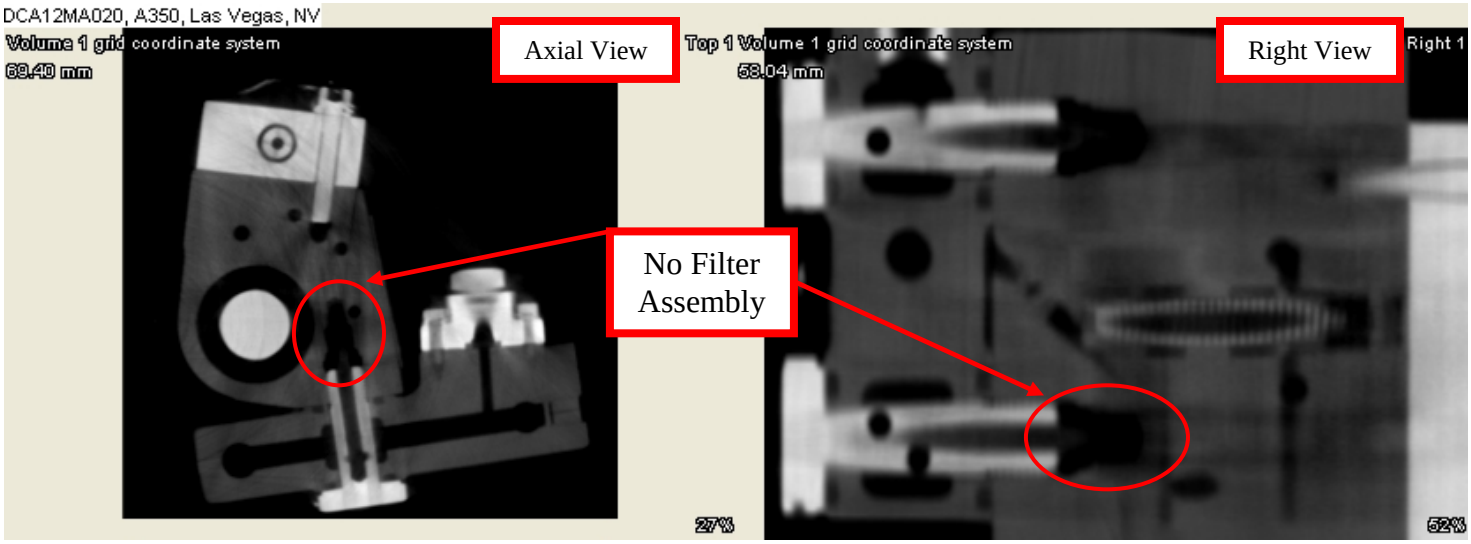

Figure 24
Multiple views – Right Lateral Actuator – Overall cross section showing the return and pressure ports and no visible filter

6.0 Computed Tomography Results – Tail Rotor Actuator

The computed tomography (CT) results for the tail rotor actuator are shown in figures 25 through 30. A total of two particles were found in various locations within the actuator.

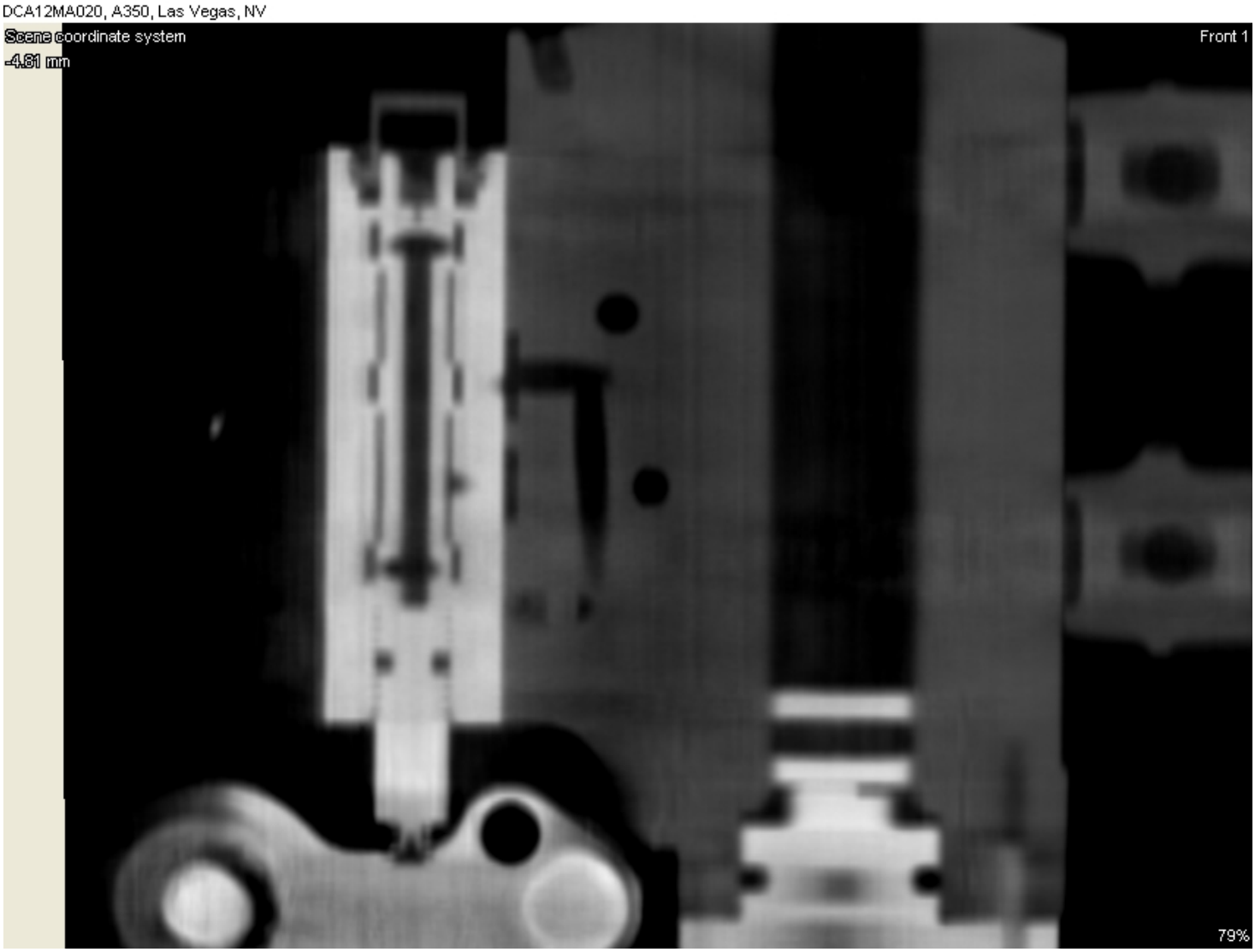

Figure 25
Frontal cross section – Tail Rotor Actuator – Overall cross section showing spool position

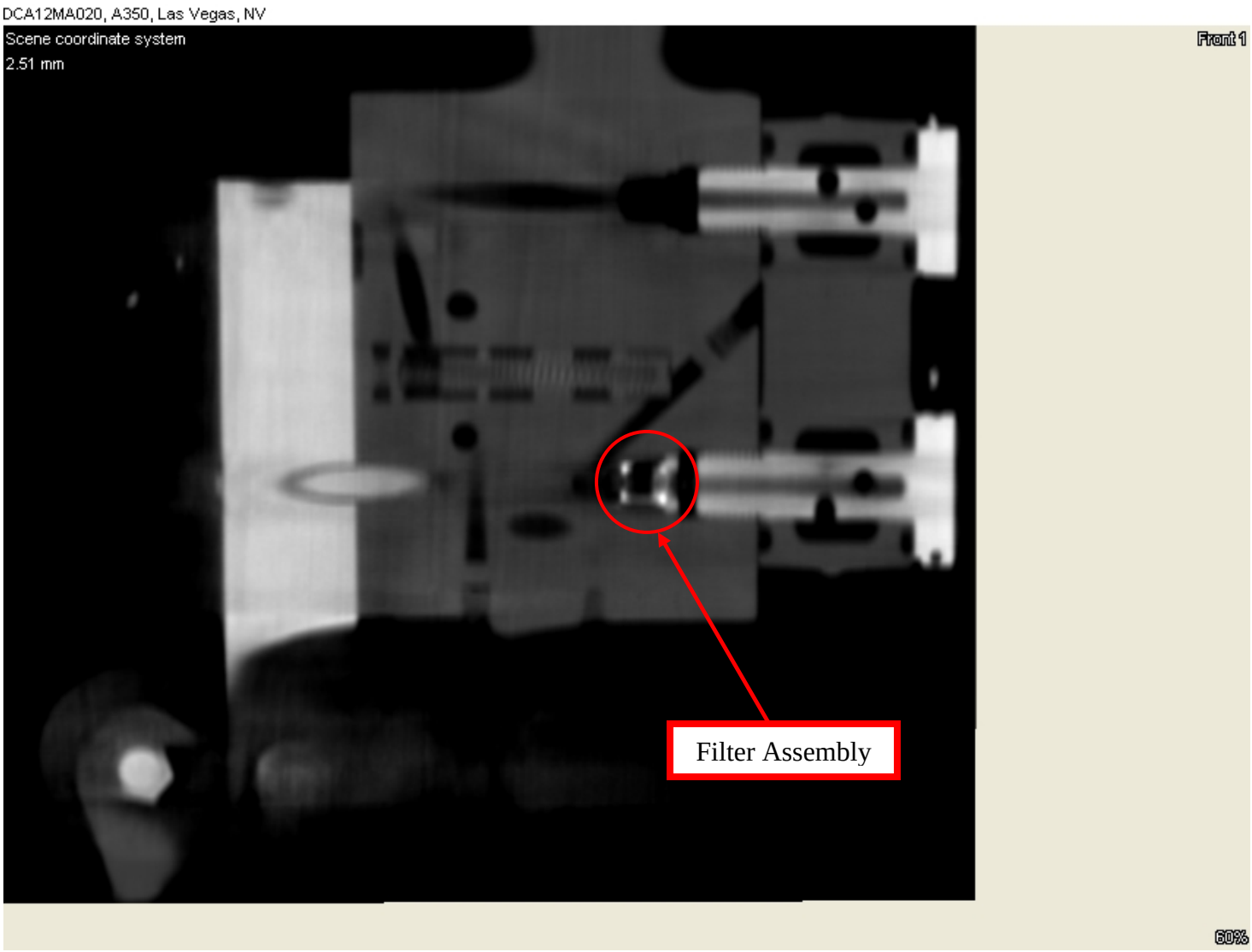

Figure 26
Frontal cross section – Tail Rotor Actuator – Overall cross section showing shuttle position and filter at the end of the pressure port

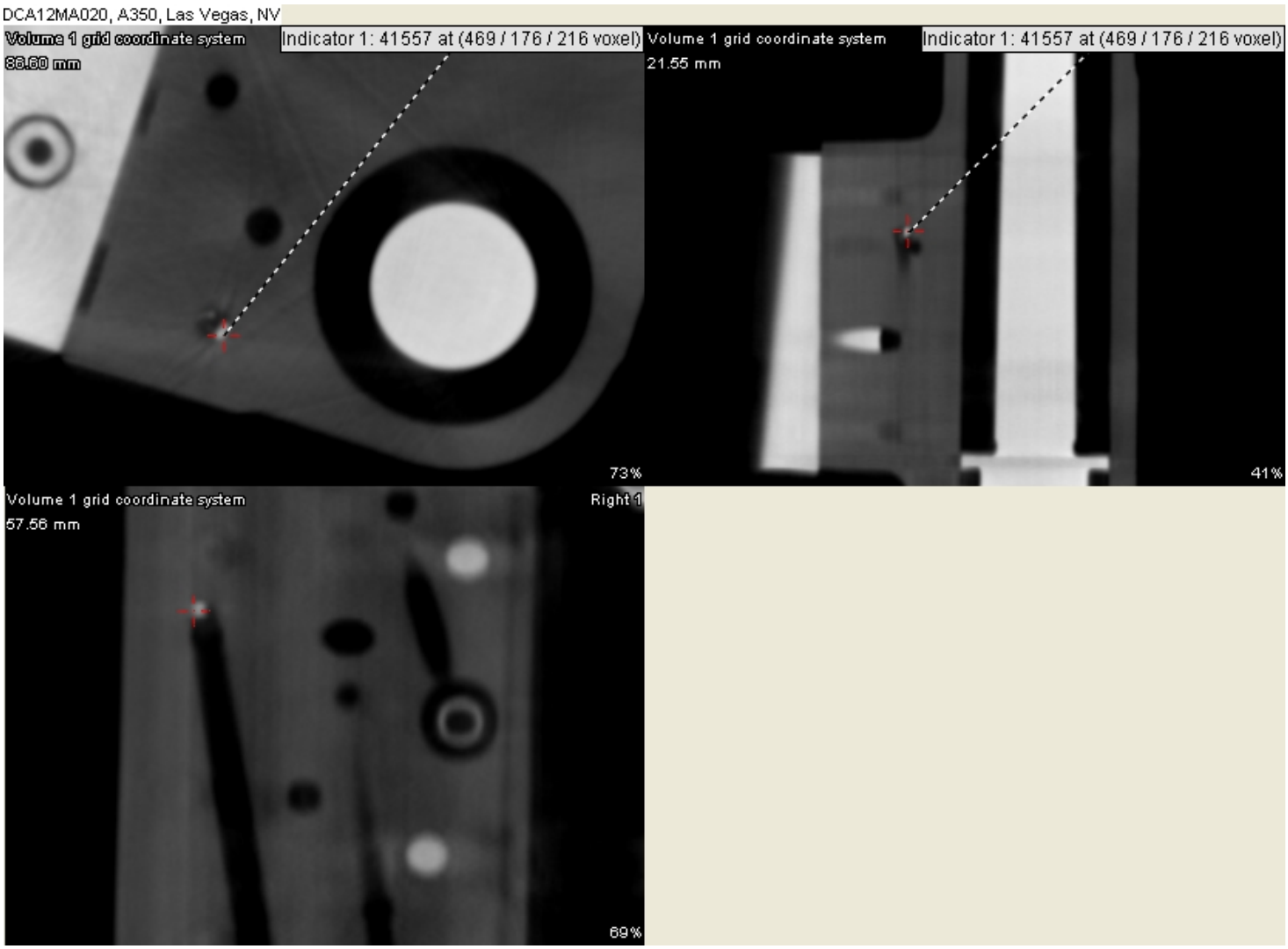

Figure 27
Multiple views – Tail Rotor Actuator – Particle 1 located at the end of a hydraulic passage

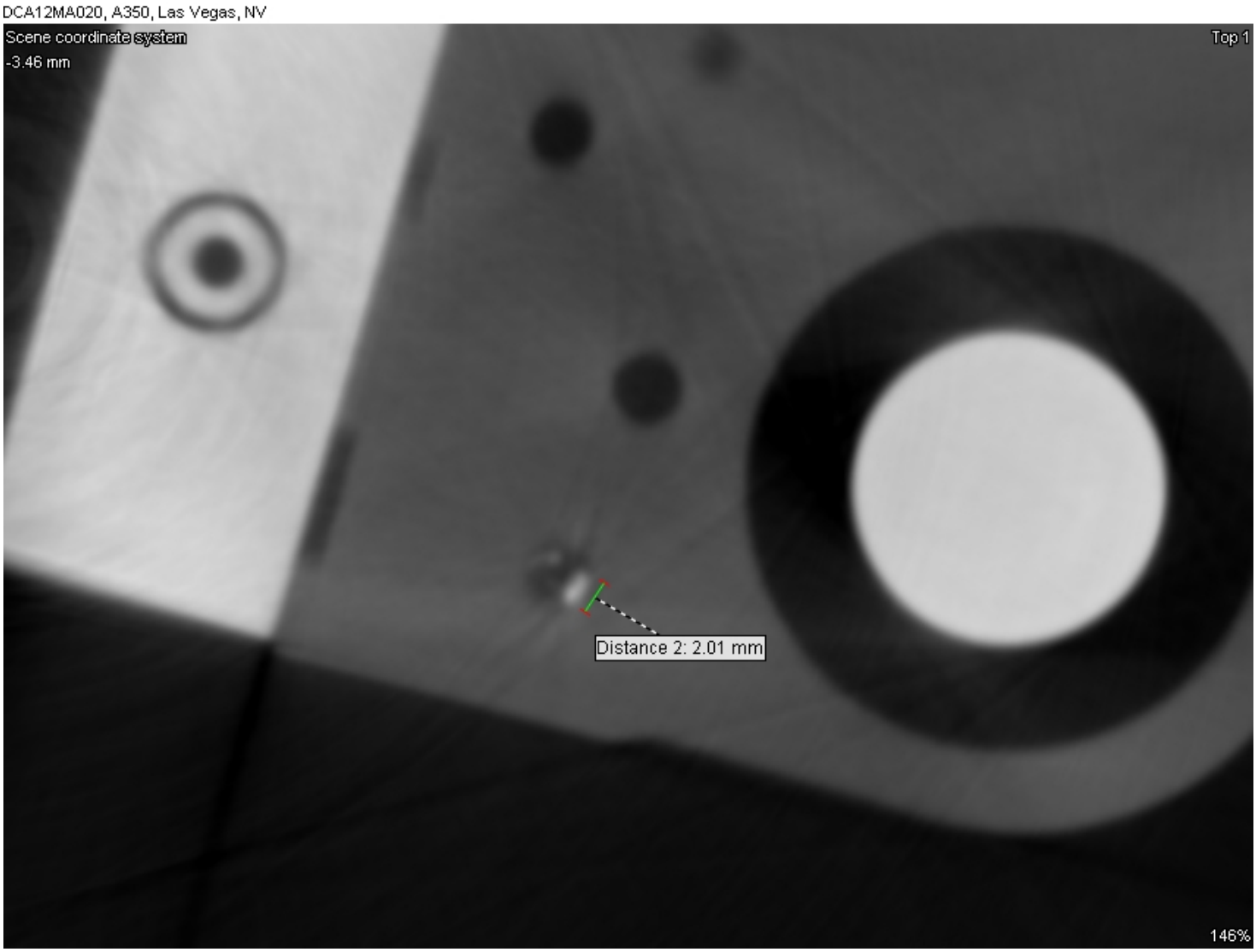

Figure 28
Axial cross section – Tail Rotor Actuator – Particle 1 (measuring 2.01 mm long) located at the end of a hydraulic passage

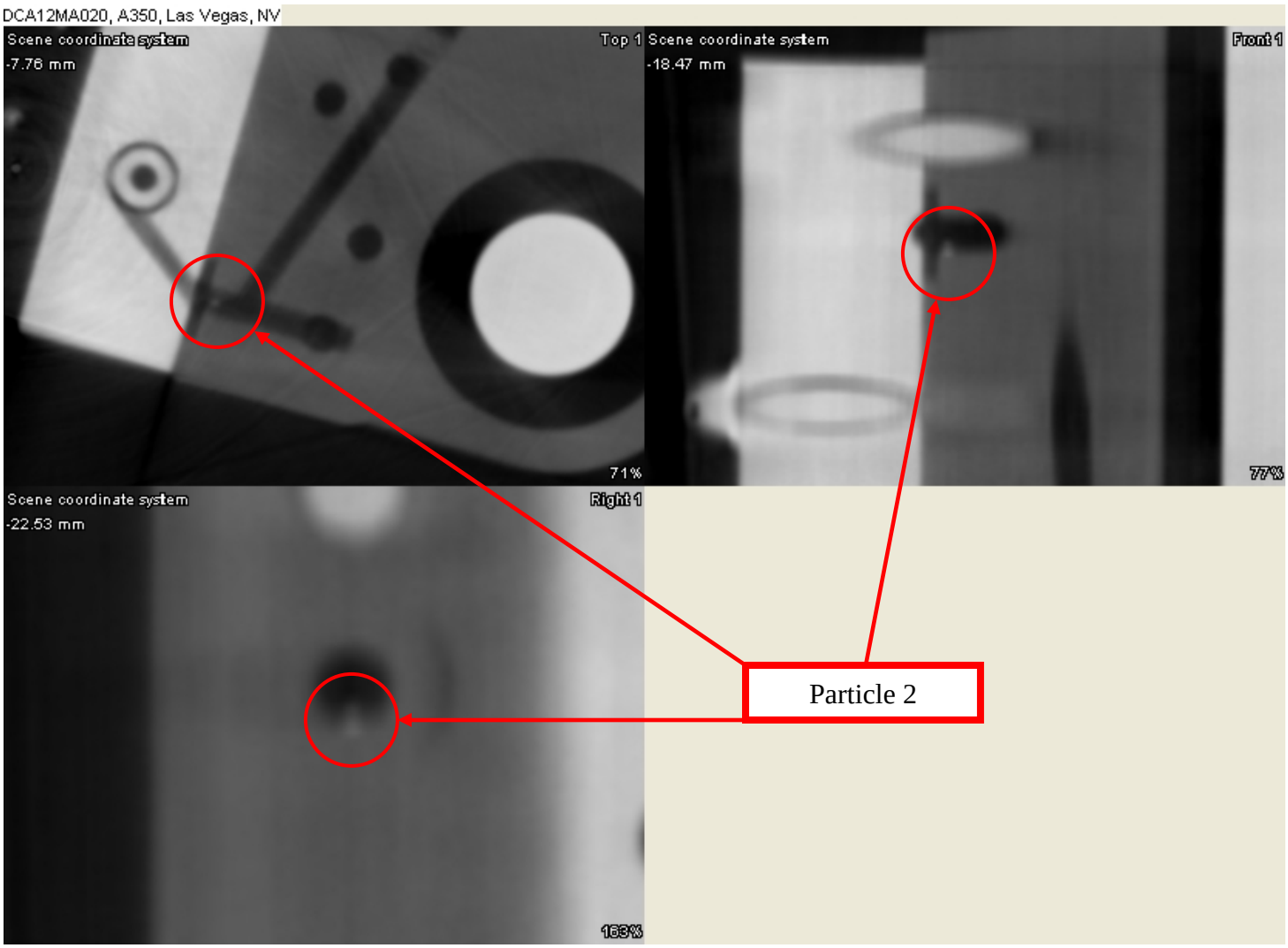

Figure 29
Multiple Views – Tail Rotor Actuator – Particle 2 located in the middle of a hydraulic passage

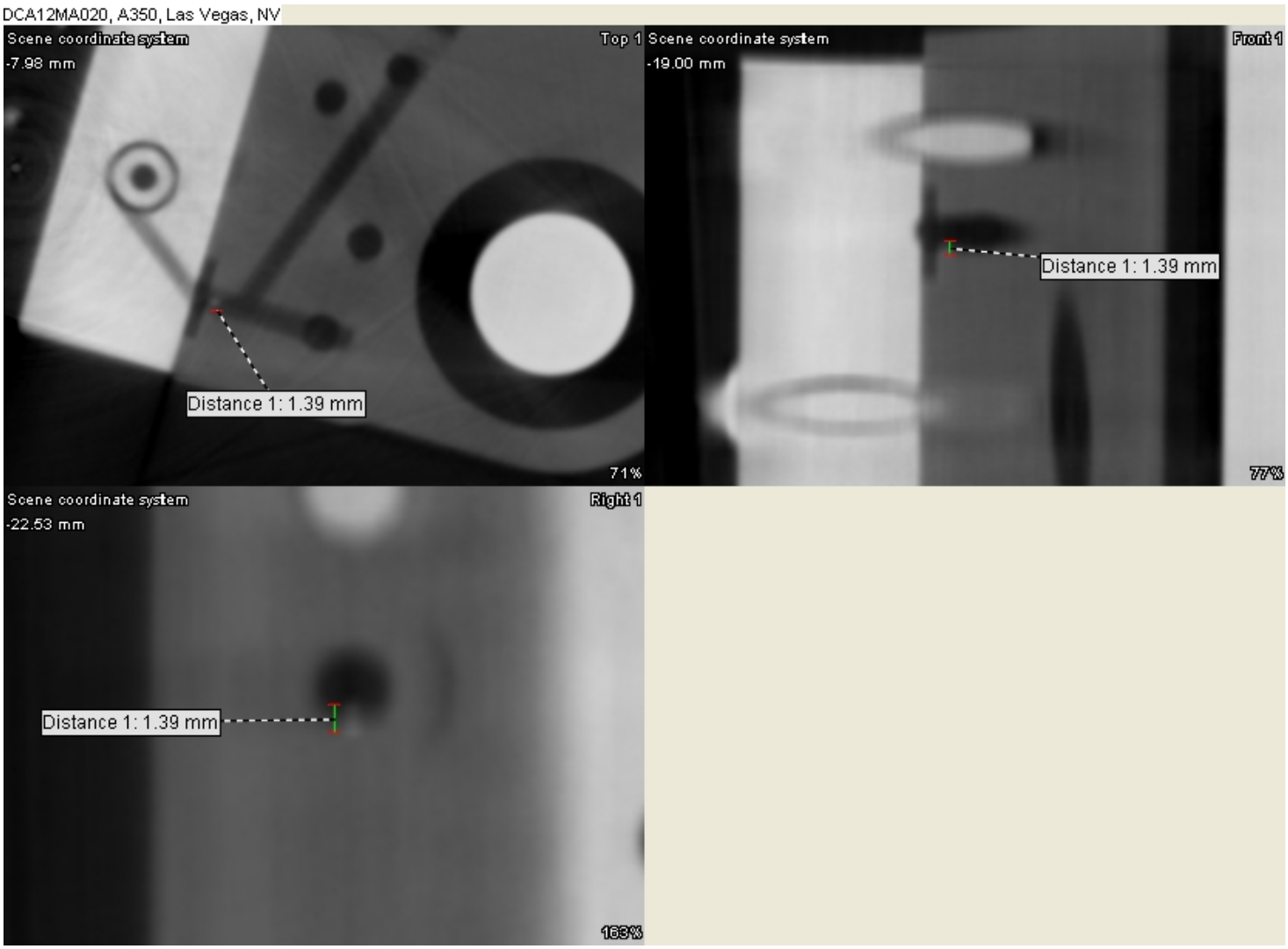

Figure 30
Multiple Views – Tail Rotor Actuator – Particle 2 (measuring 1.39 mm high) located in the middle of a hydraulic passage

7.0 Computed Tomography Results – Fore-Aft Actuator Rod End

The CT results for the fore-aft actuator rod end are shown in figure 31. There were no abnormalities noted in these CT images.

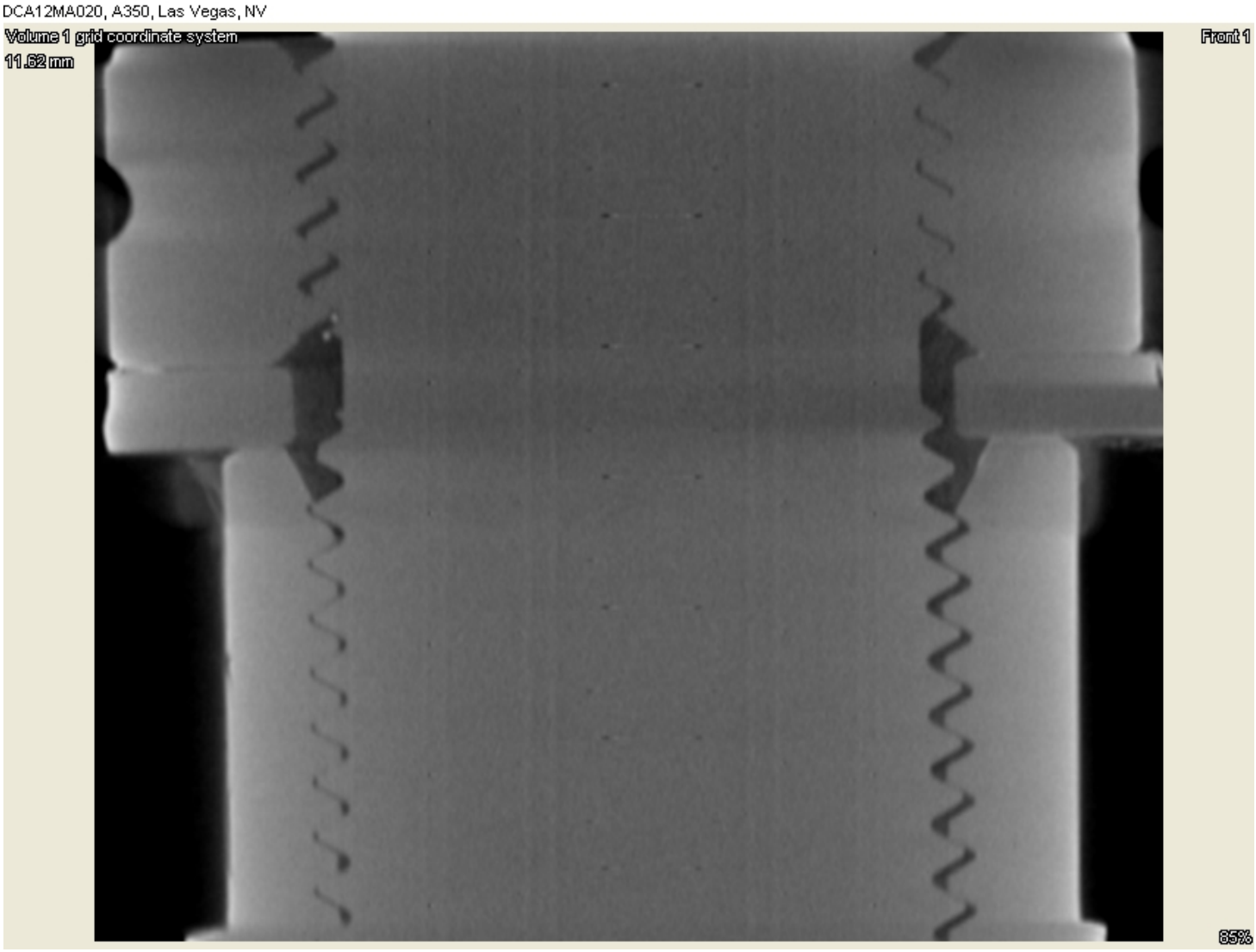

Figure 31
Frontal cross section – Fore-Aft Rod End – Overall cross section through the nut area and below

Scott Warren
Lead Aerospace Engineer
(Computed Tomography Specialist)